Combustion characteristics of HAN−based liquid propellant

Toshiyuki Katsumi*†, Hiroyuki Kodama**, Hiroyuki Ogawa***, Nobuyuki Tsuboi***, and Keiichi Hori***

*Department of Space and Astronautical Science, The Graduate University for Advanced Studies (Sokendai), 3−1−1 Yoshinodai, Sagamihara−shi, Kanagawa−ken, 229−8510, JAPAN
TEL +81−42−759−8082 FAX +81−42−759−8284
†Corresponding address : toshiyuki@isas.jaxa.jp

**Department of Chemical System Engineering, The University of Tokyo, 3−1−1 Yoshinodai, Sagamihara−shi, Kanagawa−ken, 229−8510, JAPAN

***Institute of Spaceand Astronautical Science (ISAS), Japan Aerospace Exploration Agency (JAXA), 3−1−1 Yoshinodai, Sagamihara−shi, Kanagawa−ken, 229−8510, JAPAN

Abstract

A new composition of Hydroxyl Ammonium Nitrate (HAN) based solution containing Ammonium Nitrate (AN), Methanol, and Water (H_2O) was developed for a monopropellant of reaction control system (RCS) as an alternative to conventional Hydrazine. Burning rate of the solution is moderate at operating pressures of RCS thruster. Comparing this solution with hydrazine, Isp is 20%higher, the density is 1.4 times, the freezing point is much lower, and the toxicity is low, which make this solution promising for RCS propellant.

Combustion mechanism of this solution was investigated. Burning behavior was observed using a medium speed camera, and temperature profile of combustion wave was measured with a fine ϕ2.5 microns thermocouple. From these results, the instability of liquid interface may trigger jumping of burning rate to violently high region, and methanol was found to be effective to reduce the bubble growth rate in the solution.

Keywords : Hydroxyl Ammonium Nitrate, HAN, Methanol, Combustion Mechanism, Bubble Growth

1. Introduction

HAN−based solution has been considered as candidates for a monopropellant and a liquid oxidizer of hybrid rocket because of its promise in the area of storability, environmental/health, performance, density and thermal management. However, HAN−based solutions often exhibit extremely high burning rates and such characteristics sometimes bring serious accident, which has retarded the use of the solutions to those applications. Recently, methanol addition was found to be effective to reduce the burning rate, and this study started to make the burning rate of HAN−based liquid oxidizer lower with methanol, and then found the great possibility of the HAN−based liquid oxidizer for RCS monopropellant as an alternative of hydrazine. It was found that a certain range of HAN/AN/H_2O/Methanol compositions has moderate burning rate and excellent properties in Isp, density, viscosity, melting point and reactivity with catalysts. As a monopropellant, the HAN−based solution has low toxicity and density×Isp is well above that of hydrazine.

The combustion characteristics and mechanism of HAN−based solution have been studied by several researchers for many years. B. Reed, et al.[1] evaluated the seven candidates of fuel content, which were Methanol, Ethanol, 1−Propanol, 2−Propanol, 1−Butanol, HEHN (Hydroxy ethyl hydrazine nitrate) and Glycine. As a result, methanol was selected as the best fuel content, because of the good handling, storage, ignition, and combustion characteristics. Y.

P. Chang, K. K. Kuo, et al.[2] studied the combustion characteristics of HAN−AN−Methanol−Water solutions between 0.74 and 7.3 MPa. Combustion behaviors were influenced by the content of water and methanol, and there was a change in the combustion mechanism at the pressure of the slope break point. Further, T. A. Litzinger et al.[3] proposed chemical kinetics of HAN decomposition. The eight reactions were chosen as the reduced reaction model for HAN decomposition, and the numerically simulated mass fractions of main species in both gas−phase and condensed−phase coincided with the experimental data.

Regardless of these studies, the combustion mechanism still has not been clarified completely, especially the mechanism of inducing extremely high burning rate of HAN solutions. Further, the action mechanism of methanol to reduce the burning rate is not understood fully. In our study, temperature measurements with a fine $\phi2.5$ microns thermocouple and medium speed camera observation of the combustion wave were conducted. The dependencies of the combustion wave structure upon pressure and composition were obtained. In all cases, two−phase region was observed above the liquid phase, and it was found that the color and size of bubbles changed significantly. Transient phenomena from low burning rate region to extremely high burning rate region were also observed. At a critical pressure, such large bubbles started to enter into liquid phase and the combustion wave began to propagate at extremely high burning rate. To investigate the effect of methanol to reduce the burning rate, comparison between the experimental results of the solutions with and without methanol was made. From the result of temperature measurements, it was found that the burning rate was little governed by the heat flux from gas phase flame and the burning rate may depend upon the liquid phase phenomena. Therefore, bubble growth rate which is affected by pressure and solution composition seems to be the rate−determining step. In the generality, the bubble growth is governed by the evaporation process and the successive chemical reactions. However, in this case, the effect of the latter may be small because the heat flux from gas phase flame is hardly effective to the burning rate. Evaporation rate under superheat depends upon thermophysico−chemical properties of solution, and methanol addition reduces the evaporation rate according to Van Stralen's equation[4].

2. Experimental & Results
2.1 Samples
Compositions of sample solutions are summarized in Table1.Mass ratio among HAN, AN, H_2O are fixed at 95/5/8. Sample#1does not include methanol and is originally developed as a liquid oxidizer of which melting point is below −10℃ Methanol content of sample#3 is equivalent to stoichiometric ratio against "HAN + AN"contents, thus, sample#3 indicates the highest Isp within these combinations. [Table1]

In previous study[5], linear burning rates in glass tube were measured in a strand burner purged with nitrogen gas. The burning rates of sample#1 and #3 are shown in

Table 1   sample Composition (unit : mass ratio)

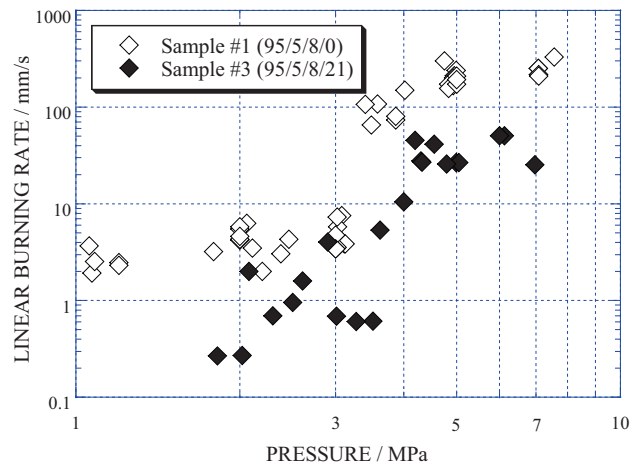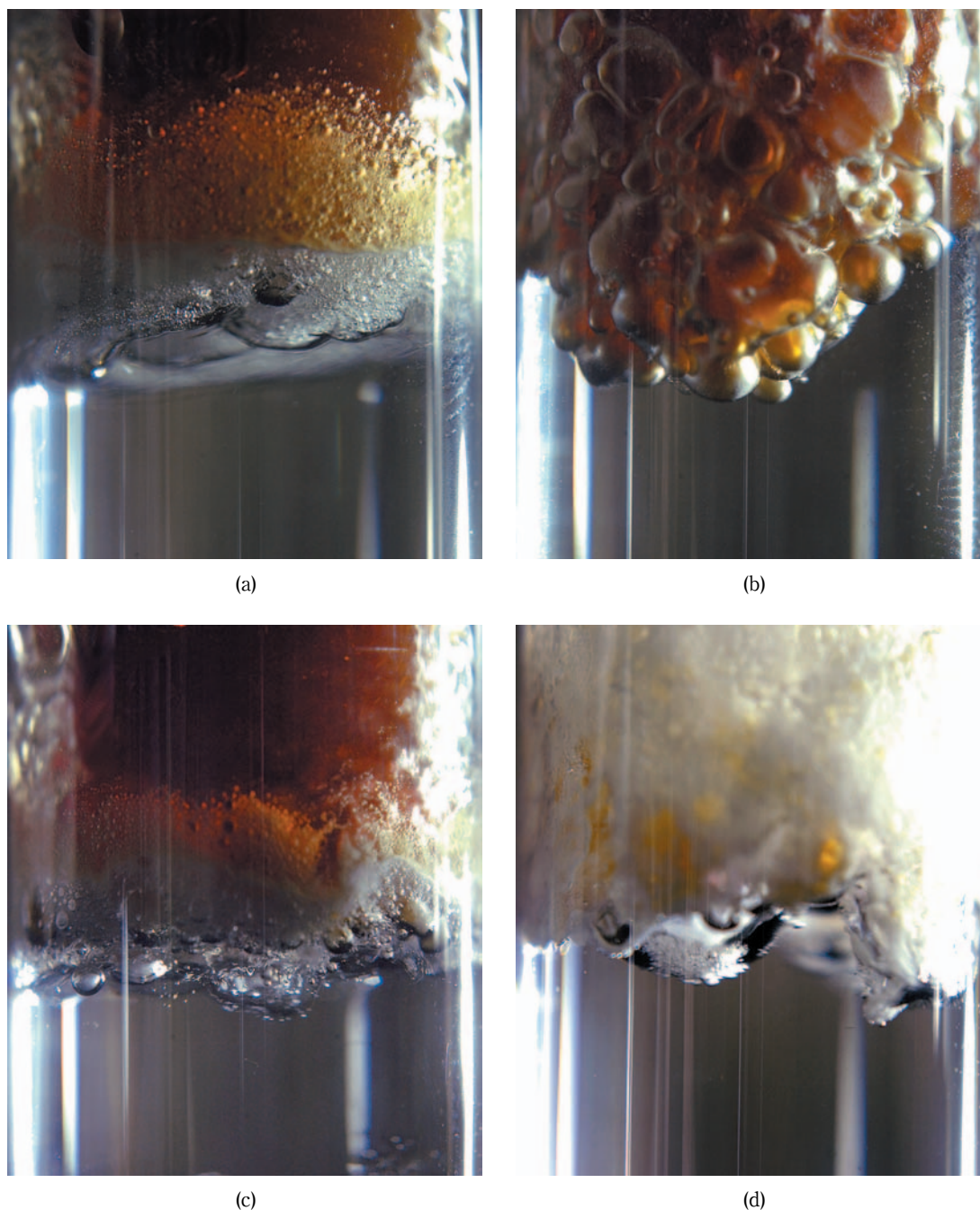| Sample	HAN	AN	H_2O	Methanol
# 1	95	5	8	0
# 3	95	5	8	21

Figure 1   Regression rate of sample

Fig.1. Sample #1 has apparently two regimes. At a certain critical pressure, regression rate jumps from moderate rate, below 10 mm s^{-1},to extremely high rate. Sample #3 has not such a critical pressure as sample #1 has, and the burning rates can be fairly lower than that of the solution without methanol especially at the operating pressures of RCS thruster, below 1.5 MPa. And, the burning rates of sample#3 below 1.5 MPa are not obtained because sample #3 has deflagration limit at around 1.5 MPa. [Figure1]

2.2 Observation of Combustion Wave
The combustion waves of HAN−based solutions in a glass tube, whose diameter was 12 mm, were recorded with a high resolution camera in a chimney type strand burner purged with nitrogen gas. And, the solution was ignited with nichrome wire. [Figure2] As shown in Fig.2(a), the burning surface of sample #1 at the low burning rate is relatively stable, and gas−liquid two−phase region is formed by the accumulation of fine bubbles just above the uniform region of liquid. The bubbles color is transparent and the thickness of the transparent bubbles is about 1.5 mm, and then, the bubbles change to brown color. In Fig.2 (b), at the high burning rate of sample #1, large and brown bubbles are observed throughout the combustion wave. In the case of sample #3, the structure of the combustion wave of Fig.2(c) at the low burning rate resembles with that of Fig.2(a). In Fig.2(d) at the high burning rate, the interface vibrates owing to the bust of large bubbles.

Transition behavior from low burning rate to high burning rate, which corresponds from Fig.2(a) to (b), was observed with the medium speed video camera at 500 fps. After the stable burning at 2.3MPa, the pressure in the burner was raised gradually on purpose. The turbulence of the gas phase was enhanced, and at a critical pressure sudden invasion of a large bubble into liquid phase was observed. This invasion triggered increasing drastically the

(a)

(b)

(c)

(d)

(a) Sample#1(rb=2.0mm/s @2.2MPa)
(b) Sample#1(rb=107mm/s @3.4MPa)
(c) Sample#3(rb=0.7mm/s @2.3MPa)
(d) Sample#3(rb=50.5mm/s @6.0MPa)
Figure 2   Photograph of the combustion wave

burning rate.

2.3 Temperature Profiles

Temperature was measured with ϕ2.5 microns S−type thermocouple in a glass tube. Representative temperature profiles are shown in Fig.3 x=0 denotes the point where the temperature rises from boiling point[6)7)]. [Figure3]

Figure3(a) is the temperature profile of sample #1, at the low burning rate (0.7mm s^{-1}@1.1MPa). As shown in Fig.3(a), temperature starts to rise from the initial temperature gradually, and there is the inflection point at the boiling point of the solvent, and then the temperature increases to the adiabatic flame temperature abruptly. In Fig.3(b), the case of sample#3, the gradient rising to the flame temperature is similar with sample #1, 6.0~7.0×10^7 K m^{-1}. Small temperature increase from −0.5 mm to 0mm of the distance in Fig.3(b) is neglected because the temperature increase is much lower than adiabatic flame temperature.

3. Discussions

The combustion mechanism of HAN−based solution based upon the experimental results is discussed here. The typical structures of combustion wave are illustrated in Fig.4. The dotted lines denote interface between liquid phase and two phase regions. [Figure4]
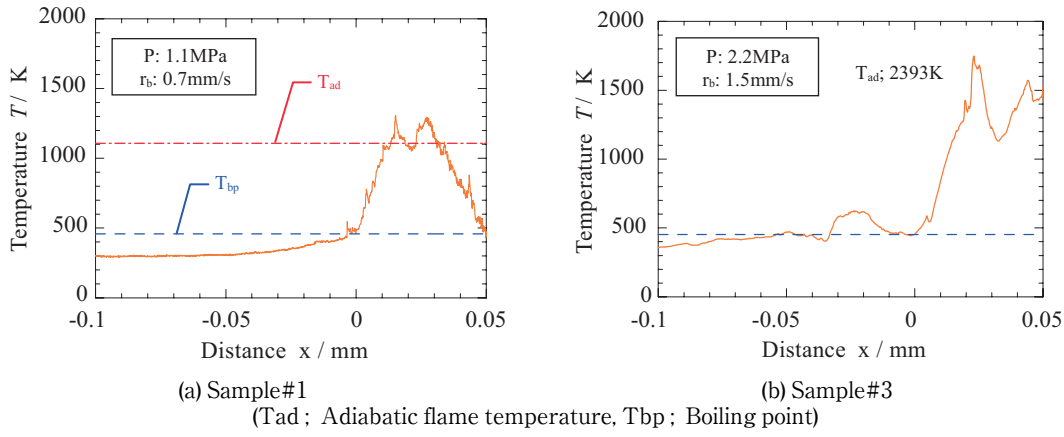
(a) Sample#1

(b) Sample#3

(Tad ; Adiabatic flame temperature, Tbp ; Boiling point)

Figure 3   Temperature profiles of the combustion wave

(i) Sample#1&#3(Low Burning Rate)
(ii) Sample#1(High Burning Rate)
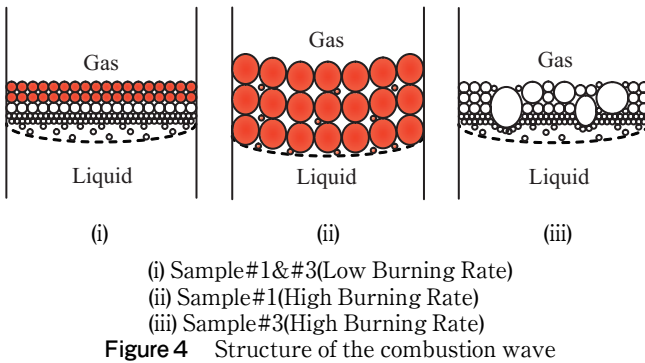(iii) Sample#3(High Burning Rate)

Figure 4   Structure of the combustion wave

The structures of combustion wave are classified into three types. As shown in Fig.4(i) at low burning rate, fine transparent bubbles are formed above the interface between liquid phase and two−phase region, and then the bubbles turn into brown color, and the product gases diffuse into gas phase. In this case, the layered structure of combustion wave may be considered as quasi one−dimensional. In fact, preheat, evaporation and combustion chemistry proceed successively and hot gases never contact directly liquid phase because there is two−phase region between hot gases and liquid phase. In Fig.4(ii) of sample #1 at high burning rate, large and brown bubbles exist throughout the combustion wave. These bubbles including hot gases propagate through liquid phase very fast. Hot gases in the bubbles contact with liquid directly and the superheat induces rapid new bubbles generation and development. Large bubbles form three dimensional interfaces between liquid phase, and this increase of interface (eventually burning surface) also contributes to the increase of the regression rate. In Fig.4(iii) of sample #3 at the high burning rate, bubble color is less dark than that in Fig.4(ii). The interface vibrates strongly, and large bubbles invade into liquid phase and new small bubbles generate as shown in Fig.4(ii), however, the new bubble growth is relatively slow. Therefore, the surface regression rate may be reduced due to the slower bubble growth rate than that in Fig.4(ii). From these results, the methanol may be effective to suppress the growth rate of small bubbles.

At low burning rate, the heat flux from gas phase flame of sample #3 is larger than that of sample #1, estimated with the temperature profile and the averaged thermal conductivity. However the burning rate of sample #3 is slower than that of sample #1. The burning rate may hardly depend upon the gas phase reaction, and the evaporation rate is considered to be the rate determining step in this case.

Evaporation carries out bubble growth, and the bubble growth rate[4] is, in general, proportional to superheat, θ, and the bubble radius, R, in a single solvent which correspond to sample#1 is expressed in the following,

$$R_1 \cong \left(\frac{12}{\pi} \right)^{1/2} \frac{(k\rho_l c)^{1/2}}{\rho_g l} \theta t^{1/2} \tag{1}$$

Here, k is liquid thermal conductivity, ρ_l is liquid density, ρ_g is gas density, c is liquid specific heat at constant pressure, l is latent heat and t is time. In the binary solution, Eq (1) is to be extended to Eq (2).

$$R_2 \cong \left(\frac{12}{\pi} \right)^{1/2} \frac{(k_m/\rho_{m,l} c_m)^{1/2}}{(\rho_{mg}/\rho_{m,l})[l_m/c_m + (k_m/\rho_{m,l} c_m D)^{1/2} \Delta T/G]} \theta t^{1/2} \tag{2}$$

$$\Delta T/G = \frac{T}{\rho_g l}(K-1)^2 p_0 x_0 \tag{3}$$

Here, Subscript m means the parameter of mixture liquid. D is mass diffusivity of more volatile component, ΔT is temperature difference between dew temperature of vapor in a bubble and a boiling point of bulk liquid in binary mixture and G is vaporized mass diffusion fraction for the individual bubble, and P_0 is ambient pressure, x_0 is mass fraction of more volatile component in originally homogeneous liquid, T is saturation temperature at ambient pressure and K is equilibrium constant of more volatile component in binary mixture. Based on the assumption that HAN and AN have small effects on the evaporation rate of solvent, $R_{2(H2O+MeOH)}/R_{1(H2O)}$ was evaluated to be approximately 0.8 at 2.2MPa.

Transition phenomena from the low burning rate to the high burning rate, which corresponds from (i) to (ii) in Fig.4, is illustrated in Fig.5. The ambient pressure was increased gradually from 2.3 MPa. Fig.5(1) shows the stable burning at 2.3 MPa (rb=3.0mm s^{-1}). Hydrodynamic instability is enhanced with increasing pressure, and the large bubbles having high temperature within them start to invade into the liquid phase (Fig.5(2)). Contacting of the hot gases included in the large bubble to the liquid generates new bubbles in the vicinity of the large bubbles. And these
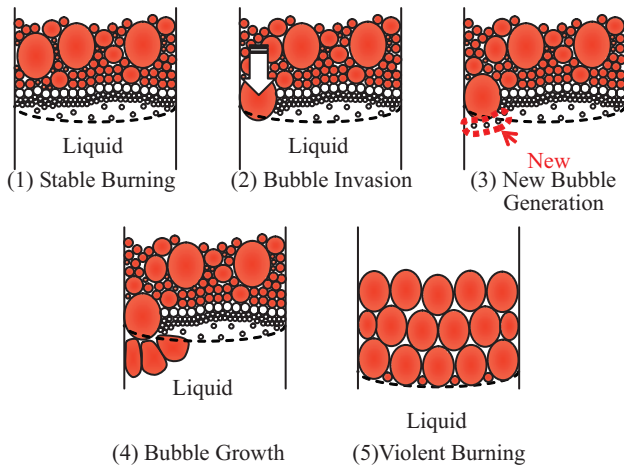
Liquid
(1) Stable Burning

Liquid
(2) Bubble Invasion

New
(3) New Bubble
Generation

Liquid
(4) Bubble Growth

Liquid
(5)Violent Burning

Figure 5   Transition process

new bubbles develop so quickly due to the severe super-heat (Fig.5(4)), and the extremely high regression rate is established in this manner (Fig.5(5)). [Figure5]

Based upon the Landau Instability theory[8)9)], the important factor for the hydrodynamic instability is inertial motion of product gases. The motion of gas in parallel direction against the surface and the local accumulation of mass enhance the motion of liquid and the instability of the liquid surface. The viscosity of product gas is effective for stabilizing, and the motion of fluid is retarded by high viscosity gas. The vapor viscosities of water and methanol are nearly same and increase with temperature. Therefore, the liquid surface will be stabilized if the temperature of the product gases is high. In the combustion of sample # 3, the flame temperature, which was obtained by the temperature measurement of combustion wave, was higher than sample #1. In addition, the average viscosity, which is estimated from the chemical equilibrium composition, of sample #3 product gases is higher than that of sample #1. For example, the viscosity of sample #3 is 0.88 mill poises when that of sample #1 is 0.48 mill poises. Thus, methanol addition should be effective to alleviate the motion of gas and stabilizes the surface.

4. Conclusions

The linear burning rate of sample #1 was reduced by the addition of methanol. The curves of pressure dependency of linear burning rate get to be smooth without critical pressure and the linear burning rates decrease at all pressures. Burning rate depends upon not the gas phase flame but the evaporation process. Methanol reduces the burning rate by the decreasing of evaporation rate and the stabilization of the liquid surface. Hydrodynamic instability is the trigger to jump into the extremely high burning rate region.

References

1) E. J. Wucherer, S. Christofferson and B. Reed, 36th AIAA/ ASME/SAE/ASEE Joint Propulsion Conference, AIAA Paper No. 2000−3872 (2000).

2) Y. P. Chang, J. K. Josten, B. Q. Zhang, B. D. Reed and K. K. Kuo, 38th AIAA/ASME/SAE/ASEE Joint Propulsion Con-ference & Exhibit, AIAA Paper No. 2002−4032 (2002).

3) H. S. Lee and T. A. Litzinger, Combustion And Flame, 135, 151−169 (2003).

4) S. V. Stralen and R. Cole, "Boiling Phenomena", Vol.1(1980), Hemisphere Publishing Corp.

5) S. Togo, K. Hori, H. Shibamoto, International Conference HEMs−2004 (2004), FGUP FR & PC ALTAI.

6) W. Yuan, A. C. Hansen and Q. Zhang, Fuel, 84, 943−950 (2005).

7) H. J. Holmes and M. van Winkle, Ind. Eng. Chem., 62, 21−31 (1970).

8) L. D. Landau, "Collected Paper of L. D. Landau", pp. 396−403 (1965), Pergamon Press.

9) Y. P. Chang, Thesis of Ph.D, pp. 234−263(2002), Pennsylvania State University.

10) H. Habu, K. Hori, T. Saito and M. Kohno, 32nd International Annual Conference of ICT, v−7(2001).

HAN系液体推進剤の燃焼特性

勝身俊之*†，児玉浩之**，小川博之***，坪井伸幸***，堀　恵一***

　硝酸アンモニウム，メタノール，および水を含むHydroxyl Ammonium Nitrate（HAN）系の新しい溶液は，従来のヒドラジンに代わる推進剤として反動推進システム（RCS）の1液推進剤として開発された．このHAN系推進剤はヒドラジンと比べて，Ispは20％高く，密度は1.4倍，氷点ははるかに低い値を示す．そして，毒性も低く，RCSの推進剤としても有望である．また，この推進剤の燃焼速度はRCSの作動圧力域で穏やかな値を示している．

　HAN系溶液の燃焼については，これまでに多くの研究者によって研究されてきたが，その燃焼メカニズムは依然明らかにされていない．本研究では，中速度カメラで燃焼の様子を観察し，燃焼波の温度場を素線径φ2.5ミクロンの極細熱電対で計測した．これらの結果に基づき，メタノールの燃焼速度抑制効果を蒸発の観点からその有効性について議論した．また，燃焼速度の急激な上昇の要因についても議論する．

*総合研究大学院大学物理科学研究科宇宙科学専攻229-8510　神奈川県相模原市由野台3-1-1
　TEL＋81-42-759-8082　FAX＋81-42-759-8284
†Corresponding address : toshiyuki@isas.jaxa.jp

**東京大学大学院工学系研究科化学システム工学専攻229-8510　神奈川県相模原市由野台3-1-1

***独立行政法人宇宙航空研究開発機構宇宙科学研究本部229-8510　神奈川県相模原市由野台3-1-1